2-1-2016

This is what COPD looks like

Khadija Sheikh

Harvey O Coxson

Grace Parraga

Official Journal of the Asian Pacific Society of Respirology
Respirology 20

INVITED REVIEW SERIES:
UNRAVELLING THE MANY FACES OF COPD TO OPTIMIZE ITS CARE AND OUTCOMES
SERIES EDITORS: GREGORY G KING AND DON SIN

This is what COPD looks like

KHADIJA SHEIKH,[1,2] HARVEY O COXSON,[3,4] GRACE PARRAGA[1,2]

[1]*Robarts Research Institute,* [2]*Department of Medical Biophysics, The University of Western Ontario, London, Canada;* [3]*UBC Centre for Heart Lung Innovation, St. Paul's Hospital,* [4]*Department of Radiology, University of British Columbia, Vancouver, Canada*

ABSTRACT

Despite decades of research, and the growing healthcare and societal burden of chronic obstructive pulmonary disease (COPD), therapeutic COPD breakthroughs have not occurred. Sub-optimal COPD patient phenotyping, an incomplete understanding of COPD pathogenesis and a scarcity of sensitive tools that provide patient-relevant intermediate endpoints likely all play a role in the lack of new, efficacious COPD interventions. In other words, COPD patients are still diagnosed based on the presence of persistent airflow limitation measured using spirometry. Spirometry measurements reflect the global sum of all the different possible COPD pathologies and perhaps because of this, we lose sight of the different contributions of airway and parenchymal abnormalities. With recent advances in thoracic X-ray computed tomography (CT) and magnetic resonance imaging (MRI), lung structure and function abnormalities may be regionally identified and measured. These imaging endpoints may serve as biomarkers of COPD that can be used to better phenotype patients. Therefore, here we review novel CT and MRI measurements that help reveal COPD phenotypes and what COPD really 'looks' like, beyond spirometric indices. We discuss MR and CT imaging approaches for generating reproducible and sensitive measurements of COPD phenotypes related to pulmonary ventilation and perfusion as well as airway and parenchyma anatomical and morphological features. These measurements may provide a way to advance the development and testing of new COPD interventions and therapies.

Key words: chronic obstructive pulmonary disease, computed tomography, imaging, phenotype, magnetic resonance imaging.

Abbreviations: 3D, three-dimensional; 4DCT, four-dimensional CT; ACOS, asthma-COPD overlap syndrome; ADC, apparent diffusion coefficient; COPD, chronic obstructive pulmonary disease; CT, computed tomography; FDMRI, Fourier-decomposition MRI; FEV1, forced expiratory volume in 1 s; FGRE, fast recalled gradient echo; FVC, forced vital capacity; HU, Hounsfield Unit; LAC, low attenuation cluster; MRI, magnetic resonance imaging; OE-MRI, oxygen-enhanced MRI; PET, positron emission tomography; PRM, parametric response maps; RA, relative area; RV, and the residual volume; SPECT, single photon emission computed tomography; TLC, total lung capacity; UTE, ultra-short echo time.

INTRODUCTION

What does chronic obstructive pulmonary disease (COPD) really look like? For years, even though our understanding of COPD has been based on global measurements of lung function, it was well-understood that disease features and phenotypes could be gleaned by 'looking' at the patient. However, in spite of this, and the fact that COPD is recognized as a heterogeneous disease with different contributions from airway[1] and parenchymal abnormalities,[2] the diagnosis and monitoring of patients and their response to therapy are currently made using airflow measurements. These measurements, while important, may conceal the independent contributions of underlying COPD pathologies especially in the early stages of disease.

Correspondence: Grace Parraga, Imaging Research Institute, Robarts Research Institute, Western University; 1151 Richmond St; London, Canada, N6A 5B7. Tel: 519-931-5265; Fax: 519-931-5238; Email: gparraga@robarts.ca

The Authors: Khadija Sheikh, BSc is a PhD graduate trainee in the Department of Medical Biophysics at Western University, London, Canada. Harvey O Coxson, PhD, is an Associate Professor of Radiology at the University of British Columbia and a Principal Investigator at the UBC Centre for Heart Lung Innovation, St. Paul's Hospital,Vancouver, Canada. Grace Parraga, PhD, is Professor and Graduate Chair in the Department of Medical Biophysics at Western University, Scientist and CIHR New Investigator, Robarts Research Institute, London, Canada.

Received 8 June 2015; invited to revise 22 June 2015; revised 24 June 2015; accepted 24 June 2015.
Article first published online: 26 August 2015

Table 1 List of technical terms and concepts

Term	Definition
Echo time	Time between MRI excitation and acquisition
Hounsfield unit	Measurement of radiodensity
Hyperpolarization	Enhancing polarization beyond thermal equilibrium conditions
Fourier transformation	An operation that decomposes a function into the frequencies
Registration	Transforming an image from one co-ordinate system to another
Segmentation	Partitioning an image into different components
Thresholding	Isolating a part of an image based on the pixel signal intensity

According to the World Health Organization, by the year 2030, COPD will be the third leading cause of death worldwide.[3] Therapies that modify COPD outcomes are still lacking and perhaps our reliance on spirometry measurements is partly responsible for this. While pulmonary function test measurements provide a straightforward and reproducible/easy to use way to measure lung function,[4] these measurements sometimes disguise or conceal different COPD phenotypes. Accordingly, one goal of COPD research is the development of ways to identify COPD patients with specific underlying pathological phenotypes with the hope that this will improve on patient care and outcomes.

In this regard, imaging methods such as chest X-ray, thoracic computed tomography (CT), single photon emission computed tomography (SPECT), positron emission tomography (PET), and magnetic resonance imaging (MRI) have played a role in the visualization of pulmonary structure and function in COPD. Quantitative imaging (i.e. imaging biomarkers) employed in research studies (but not yet clinical use), such as COPDGene,[5] ECLIPSE,[6] SPIROMICS[7] and MESA,[8] has provided repeatable and unbiased estimates of the severity and distribution of lung pathology. Here, we review novel imaging biomarkers utilized in large and small cohort studies that may help unmask the many 'faces' of COPD.

X-RAY CT

Using X-ray CT, the characterization of COPD has evolved beyond the traditional distinctions of 'emphysema' and 'chronic bronchitis' based on the presence and type of emphysema (i.e. centrilobular, panlobular, paraseptal),[9,10] the presence of bullae,[10] and their location (i.e. upper lung, lower lung, diffuse),[10] small airway disease, air-trapping, bronchial wall dilatation, wall thickening, as well as large airway disease.[11] With the introduction of clinical CT in the 1970s,[12] and with the use of computer-based image-analysis methods (summary of technical terms and concepts is provided in Table 1), the qualitative evaluation of underlying lung disease in COPD patients has matured to the evaluation of quantitative and objective regional measurements.[13]

Structural CT

Emphysema phenotypes

The CT image was originally assessed using visual scoring systems modelled after pathology. These scoring systems are still in use today, but studies have shown that they are subject to high inter- and intra-user variability.[14,15] However, the CT image is a densitometric map, where each voxel corresponds to a Hounsfield Unit (HU) value that directly reflects the radiodensity of a material. Consequently, air has a lower HU value (i.e. lower radiodensity) corresponding to lower signal intensity in a CT image and bone and tissue have relatively greater HU values because they are much more radiation absorptive. Figure 1 shows this in the axial and coronal CT images and a three-dimensional (3D) low attenuation cluster (LAC) map for an ex-smoker with emphysema-dominant COPD. The black arrows indicate large regions with mainly air (1 cm to several centimetres), or emphysematous bullae, primarily in the upper lobes. This figure also contains images from a subject that appears to have thickened airway walls and another subject that exhibits a mixture of airway wall thickening and emphysema. Quantitative analysis of the CT density histogram from these images can be done using computerized and automated methods whereby the CT density histogram of all Hounsfield unit values is evaluated using a threshold to generated the relative area (RA) of the lung occupied by attenuation values less than specific thresholds (e.g. –950HU (RA_{950}) or percentiles including the 15th percentile (HU_{15})). These measurements of emphysema correlate well with radiologists' scores,[15] pulmonary function tests[16] and histology.[17] However, an important limitation is that the threshold appropriate for emphysema is subject to image acquisition and reconstruction parameters. Moreover, the use of a single threshold can over- or under-estimate the presence of emphysema,[18] and may not be sensitive to regions with mild tissue destruction.[19]

Although these densitometric analyses (i.e. threshold-based methods) provide an unbiased measurement of emphysema severity, they do not express the regional heterogeneity of disease. One of the limitations of these methods is that the different subtypes of emphysema (i.e. centrilobular, paraseptal and panlobular), although visualized by CT, are concealed by a single number. These subtypes are typically classified based on visual assessment. Previous work has demonstrated subtype specific associations with clinical characteristics that support the notion of distinct pulmonary phenotypes according to emphysema subtype.[20]

Image analysis methods based on patterns of local features provide a way to objectively differentiate between these subtypes and some of these methods have better classification rates than expert radiologists.[21] The most straightforward of these approaches

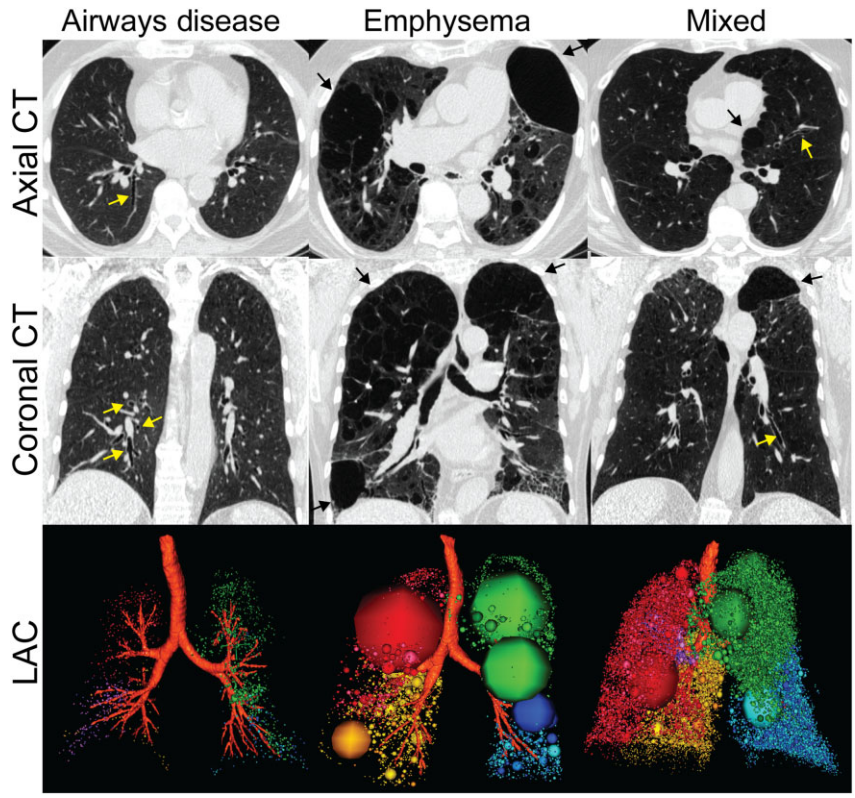

Figure 1 Structural thoracic X-ray computed tomography images. Axial and coronal CT and low attenuation clusters (LAC) of emphysema, represented as spheres with CT densitometry values below –950 HU registered to the three-dimensional reconstruction of the airway tree shown below. Yellow arrows indicate airways disease and black arrows indicate emphysematous regions. From left to right: airways disease dominant, emphysema dominant and mixed phenotype. Airways disease dominant: $FEV_1 = 103\%_{pred}$, $DL_{CO} = 119\%_{pred}$, $RA_{950} = 1\%$; Emphysema dominant: $FEV_1 = 65\%_{pred}$, $DL_{CO} = 17\%_{pred}$, $RA_{950} = 37\%$; Mixed: $FEV_1 = 47\%_{pred}$, $DL_{CO} = 62\%_{pred}$, $RA_{950} = 15\%$.

is cluster analysis, where low attenuation voxels are identified using a threshold technique and they are quantified based on how many are connected or clustered together.[22] As shown in Figure 1, the emphysema-dominant subject has large bullae in the upper lobes as identified by large clusters of CT low-attenuation regions and the subject with both emphysema and airways disease has a combination of large and small clusters distributed throughout the lung. The so-called low attenuation clusters are visually obvious, correlating with histopathology measurements[23] and more closely reflecting scoring performed by a radiologist.[24] Another method for quantifying emphysema is based on local binary patterns[25] and was shown to have a 95% classification accuracy for discriminating panlobular and centrilobular emphysema. Another approach involves principal component analysis of the CT density histogram[26] whereby a score based on each frequency–HU pair[26] is derived. While these methods may offer greater sensitivity than visual inspection, they can be difficult to integrate into clinical workflows.

Airways disease phenotypes

Airways disease in COPD patients presents with varying diagnoses and symptoms including chronic bronchitis (i.e. chronic cough vs chronic cough and phlegm) and bronchiectasis (associated with pathologic airway dilation). As shown in Figure 1, the CT image allows investigators to obtain images of airways in cross section, similar to a pathologic image or, using new techniques, create three dimensional airway trees that show the branching pattern from the trachea to the 5th or 6th generation. The yellow arrows in the axial slice indicate cylindrical bronchiectasis, whereas the arrows in the coronal view show a signet ring and varicose bronchiectasis. These images can be used to quantify airway dimensions thus providing an understanding of bronchial inflammation and remodelling and allow the stratification of disease caused by emphysematous lung destruction from airway remodelling.

Initial studies of CT airway measurements involved manually tracing the airway using the printed image. However, this process was very labour-intensive and susceptible to inter- and intra-observer error.[27] Currently, there are commercially available software packages that provide a way to reconstruct the airways from volumetric datasets (Fig. 2, Pulmonary Workstation V.2.0 VIDA Diagnostics, Coralville, Iowa, USA). These software tools and others (e.g. Thoracic VCAR (General Electric Healthcare, Milwaukee, USA), Apollo Image analysis software (VIDA Diagnostics), Mimics Innovation Suite (Materialise, Leuven, Belgium), Pulmo3D Software (Fraunhofer MEVIS, Bremen, Germany), Airway Inspector (Harvard Medical School, Boston, MA) and 3D SLICER (http://www.slicer.org, Boston, MA)) allow for the quantification of luminal diameter and wall thickness to the fifth or sixth airway generation. Indices of airway dimensions include total bronchial area, bronchial luminal area, bronchial wall thickness and area and the per cent of the total bronchial area that is wall area per cent (WA%).[28] Another measure of bronchial wall area (or thickness) that was developed to try and

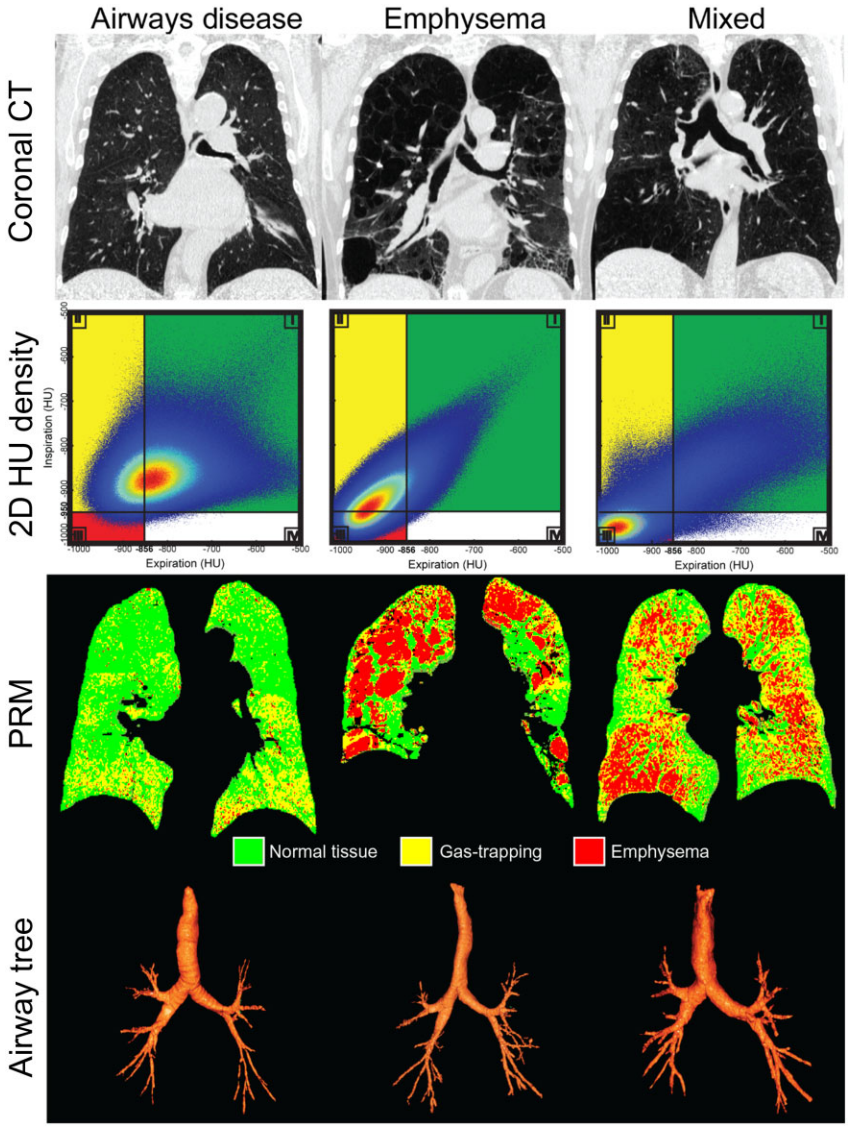

Figure 2 Functional thoracic X-ray computed tomography images. Coronal CT, Hounsfield Unit density plots, parametric response maps (PRM), and reconstructed CT airway trees are shown below. From left to right: airways disease dominant, emphysema dominant and mixed phenotype. Airways disease dominant: WA = 64%, PRM Normal Tissue = 73%, PRM Gas Trapping = 26%, PRM Emphysema = 1%; Emphysema dominant: WA = 63%, PRM Normal Tissue = 42%, PRM Gas Trapping = 17%, PRM Emphysema = 38%; Mixed: WA = 59%, PRM Normal Tissue = 28%, PRM Gas Trapping = 47%, PRM Emphysema = 24%.

alleviate the error in the WA% caused by measuring small airways, is the square root of wall area of an idealized airway with an internal perimeter of 10 mm (Pi10),[29] which is calculated using a linear regression of all measured bronchi.

One of the first studies of airway dimensions demonstrated that WA% correlated with the forced expiratory volume in 1 s (FEV_1), forced vital capacity (FVC), and the residual volume/total lung capacity (RV/TLC), but not DL_{CO}.[30] Since then, studies have shown that airway wall measurements are associated with histology,[29] frequency of exacerbations[31] and dyspnea.[32] Previous studies also examined subjects with COPD and the clinical diagnosis of chronic bronchitis and determined that subjects with chronic bronchitis and COPD had thicker airway walls than those without chronic bronchitis and COPD.[33] Recent work showed that quantitative CT measures of airway thickness in COPD patients were greater in those with bronchodilator responsiveness.[34] Most of the studies published to date tend to take all the airway measurements and use them together as a single global measurement. However, a recent study suggests that airways need to be described in terms of their anatomic location[35] and according to number of generations from the trachea. This approach showed that in some COPD patients, airway walls become thinner and not thicker. A previous study also compared airway measurements in patients with asthma-COPD overlap syndrome (ACOS) and those with COPD patients and demonstrated that subjects with ACOS had significantly higher WA%, but similar emphysema scores.[36] To date, these analytical approaches have not revealed strong correlations between lung function and CT measurements of emphysema and airway wall remodelling, and this is very likely because there are very few, if any, patients with exclusively one phenotype. Most subjects with moderate disease report a mixture of airway wall abnormalities and parenchymal destruction, and it emphasizes the point that the lung needs to be

assessed regionally and global measurements miss both functional and anatomic changes.

Finally, it should also be recognized that the use of CT to quantify and classify emphysema and airways disease severity can be challenging. For example, inconsistent scanning and image reconstruction parameters[37] and poor coaching of the patient to the targeted lung volume[38] are some of the image acquisition issues that limit more widespread use.

Functional CT

Pairing regional structural and functional information is critical for understanding the aetiology of COPD. By understanding the emphysema and airway components without tying these to functional consequences, we remain blind to the variations in pulmonary perfusion and ventilation and, more importantly, the complete picture of COPD. Thus, by taking into account the functional changes that accompany structural changes, we will be one step closer to comprehensive individualized disease characterization.

Gas trapping and ventilation phenotypes

Conventional CT is limited to the evaluation of lung parenchyma and airway abnormalities. However, recently, investigators have started to use CT images acquired at both end inspiration and expiration to try and assess low attenuation areas due to emphysematous destruction and air-trapping related to small airway disease.[5] Investigators have taken this a step farther and have co-registered the inspiratory and expiratory CT images to generate parametric response maps (PRM), to further describe low attenuation areas on the CT scans as emphysematous or due to gas trapping because of small airway disease, termed 'functional small airway disease' (Fig. 2). As shown in the PRM maps provided in Figure 2, the airways disease dominant COPD subject has regions of gas trapping in the lower lobes (indicative of small airways disease) and no obvious regions of emphysema. The subject with emphysema dominant COPD has obvious bullous regions, and the subject with the mixed phenotype has contributions from both small airways disease and emphysema. In comparison to the anatomical coronal CT slices shown, the PRM maps allow for the regional quantification of gas trapping and emphysema. These PRM measurements of gas trapping and emphysema have been shown to be associated with pulmonary function tests, quality of life questionnaires and frequency of exacerbations.[39]

Pulmonary function has also been evaluated using xenon-enhanced dual-energy CT. Dynamic CT images are acquired during the wash-in of xenon gas during inhalation or wash-out of xenon gas during exhalation. This work showed that there was an inverse relationship for xenon gas wash-out with lung function[40] and point to the relationship between trapped gas or slow emptying units and conventional pulmonary function measurements. Thoracic imaging functional maps and measurements are possible using four-dimensional CT (4DCT).[41] Originally developed for radiotherapy treatment planning, 4DCT allows for the acquisition of the 3D image throughout the respiratory cycle. Although good agreement between ventilation MRI and 4DCT has been demonstrated in lung cancer patients,[42] because of radiation dose, 4DCT is not suited for longitudinal monitoring of COPD. Alternative methods have emerged for the acquisition of thoracic images at multiple lung volumes without contrast agents. For example, a two-lung volume (TLC and RV) CT protocol has been standardized as part of the 'SPIROMICS'[7] study. Using this approach in combination with advanced image registration methods,[43] lung ventilation maps may be generated and evaluated.

Perfusion phenotypes

In COPD patients pulmonary abnormalities stem from inflammatory processes, triggered by inhaled noxious particles. Remarkably, in about half of smokers, the inflammatory process is self-repairing; however, in the remainder, inflammation results in airway and parenchymal abnormalities.[44,45] Importantly, hypoxic pulmonary vasoconstriction is normally blocked in the presence of inflammation.[46] To ascertain the influence of inflammation on pulmonary perfusion, dynamic CT methods have been used to measure blood flow and mean transit time.[47,48] This work showed that early or mild emphysema is characterized by heterogeneous pulmonary perfusion possibly due to inflammation.[49] Moreover, CT-perfusion studies suggested that blood flow is diminished to inflamed lung regions in patients with emphysema.

MAGNETIC RESONANCE IMAGING

Although pulmonary MRI remains technically challenging due to the unique characteristics of lung tissue, MRI using hyperpolarized noble gases and conventional methods has helped to change our understanding of COPD.

Proton MRI phenotypes

MRI of the lung is demanding for several reasons. First, the lung parenchyma is predominately composed of alveolar ducts and alveoli, which are air-filled, and thus very little ^{1}H signal that can be detected from the small amount of tissue present. Second, the lung parenchyma also has a short transverse magnetization relaxation time, known as T_2, and consequently a short T_2^* which is the sum of the T_2 relaxation time and an additional field inhomogeneity term. This magnetic property of the lung results in a much faster MR signal decay for the lung parenchyma in comparison to other tissues. Third, the air and tissue have very different magnetic properties and the air–tissue interfaces, such as those at the alveolar membrane, result in magnetic field gradients that may further degrade the ^{1}H signal and distort the image.

Proton MRI anatomical and microstructural imaging

Although hampered by low signal intensity, pulmonary ^{1}H MRI can be performed on conventional

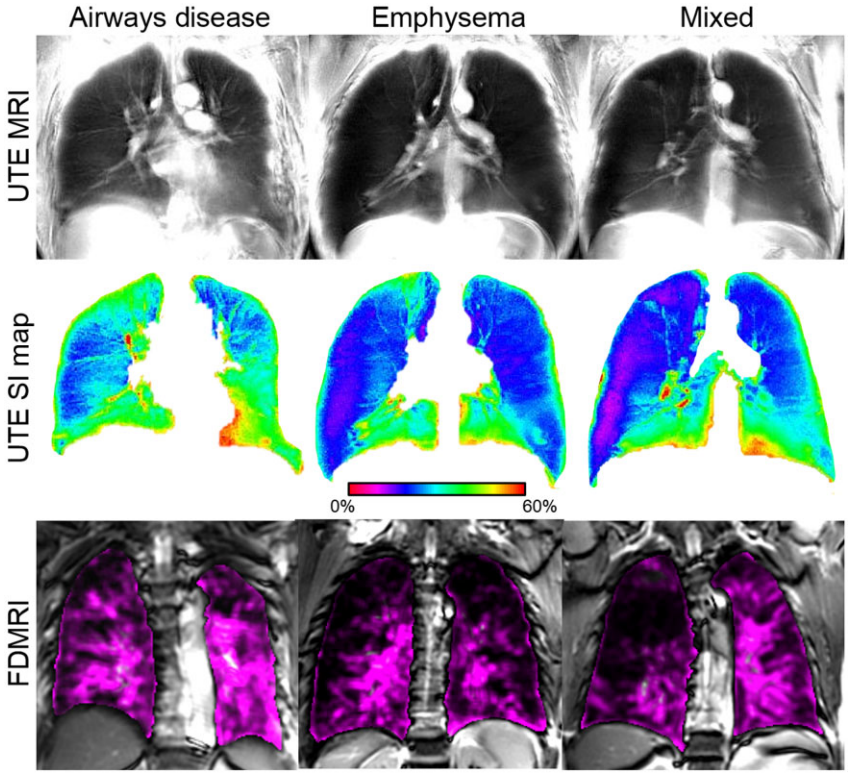

Figure 3 ^{1}H MR images acquired using fast recalled gradient echo (FGRE), ultra-short echo time (UTE) and Fourier Decomposition MRI of subjects shown below. From left to right: airways disease dominant, emphysema dominant and mixed phenotype. Airways disease dominant: $FEV_1 = 89\%_{pred}$, $DL_{CO} = 64\%_{pred}$, $RA_{950} = 2\%$, ^{1}H UTE signal-intensity = 29%; Emphysema dominant: $FEV_1 = 28\%_{pred}$, $DL_{CO} = 32\%_{pred}$, $RA_{950} = 37\%$, ^{1}H UTE signal-intensity = 22%; Mixed: $FEV_1 = 52\%_{pred}$, $DL_{CO} = 55\%_{pred}$, $RA_{950} = 28\%$, ^{1}H UTE signal-intensity = 22%.

scanners without a great deal of physics support. For example, methods have been devised that combine relaxation signals and intravenous contrast to differentiate inflammation,[50] smooth muscle remodelling, oedema and mucus deposition.[50,51] Conventional ^{1}H MRI allows for the visualization and quantification of emphysema,[52] the differentiation of oedema from mucous deposition[50,51] and the differentiation of emphysema from mucous plugs[53]; these findings point to the potential of ^{1}H MRI to help unmask the many faces of COPD.

Recent technical advancements using short and ultra-short echo time (UTE) acquisition methods help address the inherent challenges of low tissue and ^{1}H density[54] by minimizing the effects of rapid MR signal decay. Figure 3 shows ^{1}H UTE MR signal intensity maps of three representative COPD subjects. For signal intensity maps, cool colours represent regions of low signal intensity (or diminished tissue density such as in emphysema) and the warmer colours represent regions of high signal intensity (or high tissue density such as in bronchiectasis or airways disease). The emphysematous and mixed phenotype subjects have obvious regions of low signal intensity, while in contrast, the subject with mainly airways disease has regions with greater signal intensity. The relationship between MRI signal intensity and tissue density, as previously shown for pulmonary CT, is clearly important for further development of the method. The first studies employing UTE methods reported that the tissue density was related to MR signal[55] and T_2*. More recently, UTE MRI was implemented to measure signal intensity and T_2* in emphysema[56] and showed good correlations with histological measurements. UTE MRI in COPD patients also showed that T_2* correlated with pulmonary function measurements[52] and pulmonary signal intensity was related to tissue density, pulmonary function and CT density measurements.[53] The longitudinal relaxation time (T_1) may be used to characterize COPD patients with emphysema[57] because there is a shorter lung T_1 in emphysematous tissue than in fibrosis, suggesting that the T_1 relaxation time may directly reflect tissue density.

Proton MRI lung function imaging: ventilation and perfusion

Recently, free-breathing Fourier-decomposition MRI (FDMRI) was developed as a way to generate regional ventilation and perfusion maps. Importantly FDMRI does not require tracer gases because it takes advantage of the very weak but native contrast generated when air enters and leaves the lung during normal tidal breathing.[58] During a short 2-min scan, both ventilation (shown in Fig. 3 for three COPD patients) and perfusion maps can be generated to evaluate ventilation/perfusion mismatch in COPD patients. As shown in Figure 3, regions of signal void represent 'ventilation defects' that spatially correlated with inhaled gas MRI ventilation defects and bullae.[59] Clearly, the time constants for filling and emptying the lung may explain the lack of ventilation in some regions of the lung. Currently, FDMRI utilizes a short-echo method[60] available on most clinical scanners and can be rapidly performed without exogenous inhaled gases. This opens up more widespread

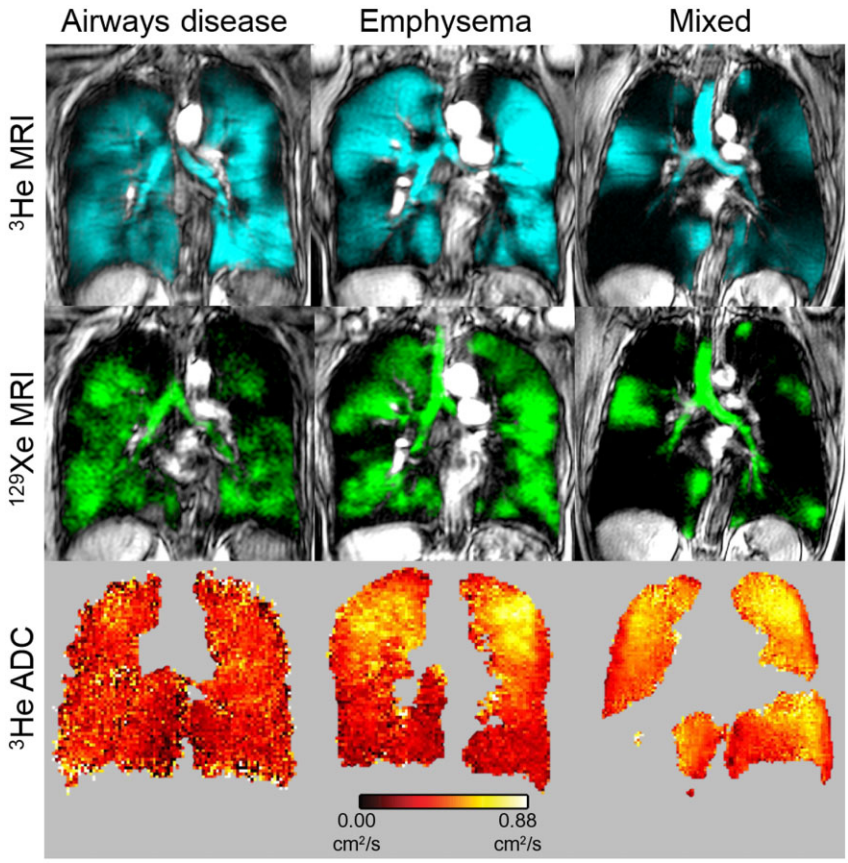

Figure 4 Hyperpolarized noble gas MR images. ^{3}He and ^{129}Xe static ventilation and ^{3}He ADC images shown below. From left to right: airways disease dominant, emphysema dominant and mixed phenotype. Airways disease dominant: VDP = 8%, ADC = 0.32 cm^2/s; Emphysema dominant: VDP = 12%, ADC = 0.40 cm^2/s; Mixed: VDP = 45%, ADC = 0.42 cm^2/s.

opportunities for functional lung imaging of COPD patients on clinical (and not just research) MR systems.

Oxygen-enhanced MRI phenotypes

Oxygen-enhanced MRI (OE-MRI) takes advantage of the physical properties of molecular oxygen resident in the lung. When dissolved in blood, molecular oxygen shortens the T_1-relaxation time of the pulmonary venous blood, and this translates to an increase in MR signal[61] that is dependent upon the presence of O_2 itself. To acquire such images, subjects first breathe in room air (21% oxygen) for imaging, then 100% oxygen for a short period of time and then room air again to generate difference maps. In this manner, O_2-enhanced maps may be generated as per cent change maps from the oxygen-enhanced and room air images.[62] In a comparison of smokers with and without COPD, OE-MRI measurements were correlated with smoking history, lung function and CT measurements. Significant relationships between diffusing capacity for carbon monoxide and signal intensity derived from OE-MRI were also shown.[63] Taken together, this work suggests that OE-MRI has potential for evaluating pulmonary function in COPD patients.

Inhaled gas contrast MRI phenotypes

Ventilation phenotypes

Currently, hyperpolarized noble gas MRI using inhaled ^{3}He and ^{129}Xe gas provides the most common way to visualize and quantify ventilation (Fig. 4).[19] ^{19}F MRI has also recently emerged as a ventilation imaging alternative to hyperpolarized gas MRI[64] with the advantage that perfluorinated gases do not require any extra polarization.[65] Using any of these ventilated MRI methods, and as shown in Figure 4, regions of the lung that are not ventilated during inhalation are revealed as a signal void.[66] MRI ventilation imaging also revealed significant bronchodilator responses in COPD patients (similar in asthma[67]), not reflected by FEV_1. Figure 5 shows two representative COPD subjects with and without an imaging bronchodilator response. The ventilation defects are visually reduced post-salbutamol in one COPD subject similar to what is shown in the asthmatic subject. The functional information obtained using MRI may help us understand the clinical differences between ACOS and COPD and help guide therapy. Ventilation defects are also a unique predictor of exacerbations[68] in patients with mild disease in whom FEV_1 and previous exacerbations was not prognostic. As shown in Figure 4, the distribution of ventilation defects varies for patients with airways-disease dominant, emphysema dominant or mixed airways disease and emphysematous disease.[69]

Parenchyma phenotypes

In addition to the visualization of gas distribution, there is also the potential to measure parenchyma integrity. To enable this, methods have been developed that are sensitive to ^{3}He gas Brownian motion. The ^{3}He apparent diffusion coefficient (ADC) reflects

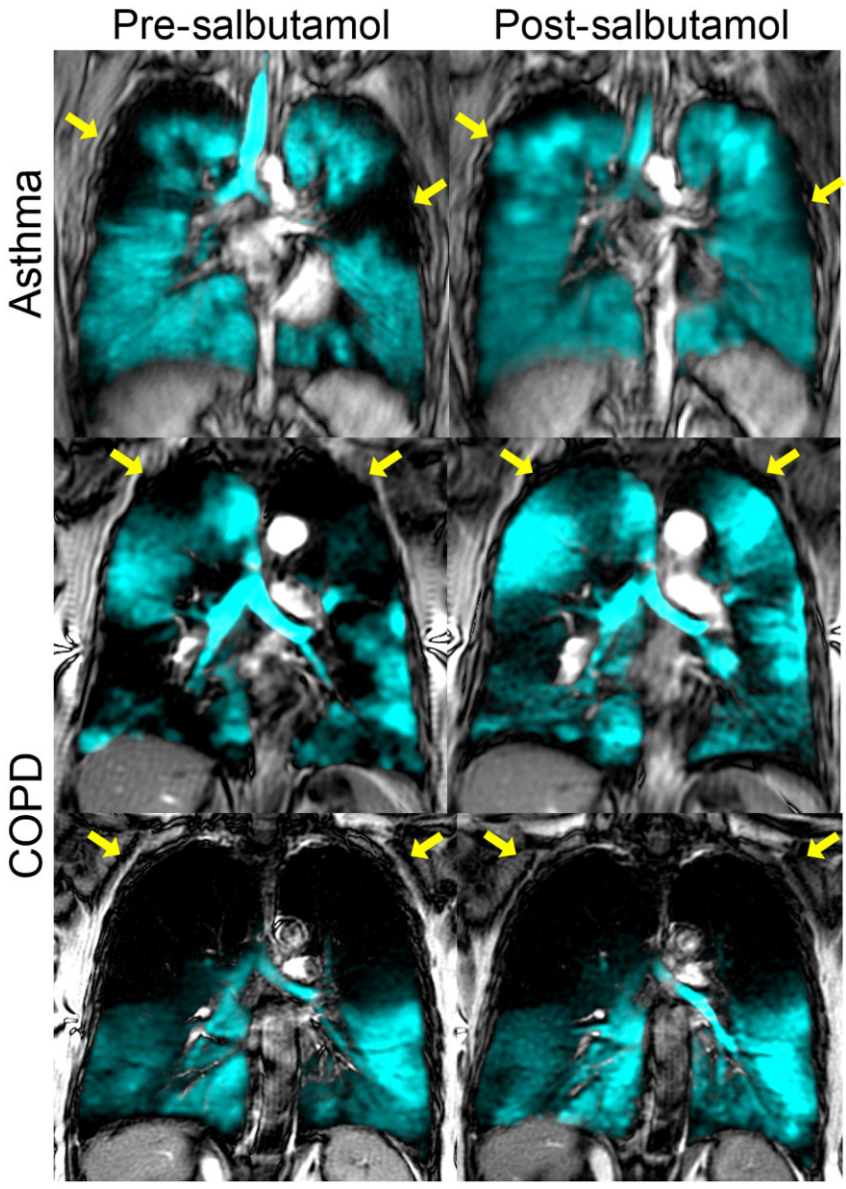

Figure 5 Hyperpolarized ^{3}He ventilation maps pre- and post-salbutamol for a representative asthmatic subject (32 year old female, pre-FEV_1 = 33%$_{pred}$ and post-FEV_1 = 50%$_{pred}$), and COPD subjects with (73-year-old female, pre-FEV_1 = 61%$_{pred}$ and post-FEV_1 = 75%$_{pred}$) and without (74-year-old female, pre-FEV_1 = 50%$_{pred}$ and post-FEV_1 = 51%$_{pred}$) imaging bronchodilator response.

the distance that a He molecule can move within the airspaces of the lung. These measurements showed that ex-smokers with and without COPD report significantly elevated ^{3}He ADC values compared to healthy volunteers, reflecting larger airspaces related to emphysema. The ADC value is attractive because it correlates with histological measurements of airspace size[70] and is more sensitive than stereology measurements to regional emphysema. ADC values have also been correlated with pulmonary function test measurements,[71] age[72] and smoking history.[72] Studies in asymptomatic smokers[73] and ex-smokers without COPD[74] have elevated ADC measurements, suggesting that the ADC is a sensitive measure of lung tissue destruction not obvious using CT[73] or reflected by self-reported symptoms.

Hyperpolarized ^{129}Xe MRI in healthy volunteers and COPD patients has been reported[75,76] but more importantly ^{129}Xe MRI has the capacity to generate perfusion images because of the solubility of ^{129}Xe in tissues and blood. This was exploited using radioactive Xe and allowed physiologists to describe ventilation and perfusion patterns in the lung.[77] Another very important feature of ^{129}Xe is that MR frequency of Xe shifts as the molecule moves from the airspace to tissue and blood. This provides a way to track the kinetic profile of Xe atoms from the gas phase across the alveolar membrane and into blood.[78]

Inhaled gas MRI has also been exploited to estimate the geometry within the alveolar space itself.[79] This approach, first pioneered using ^{3}He,[79–81] and then implemented using ^{129}Xe,[82] can be used to estimate alveolar length, external airway radii, internal airway radii and alveolar sheath size. In a similar fashion, inert ^{19}F ADC in rats[83] and excised healthy

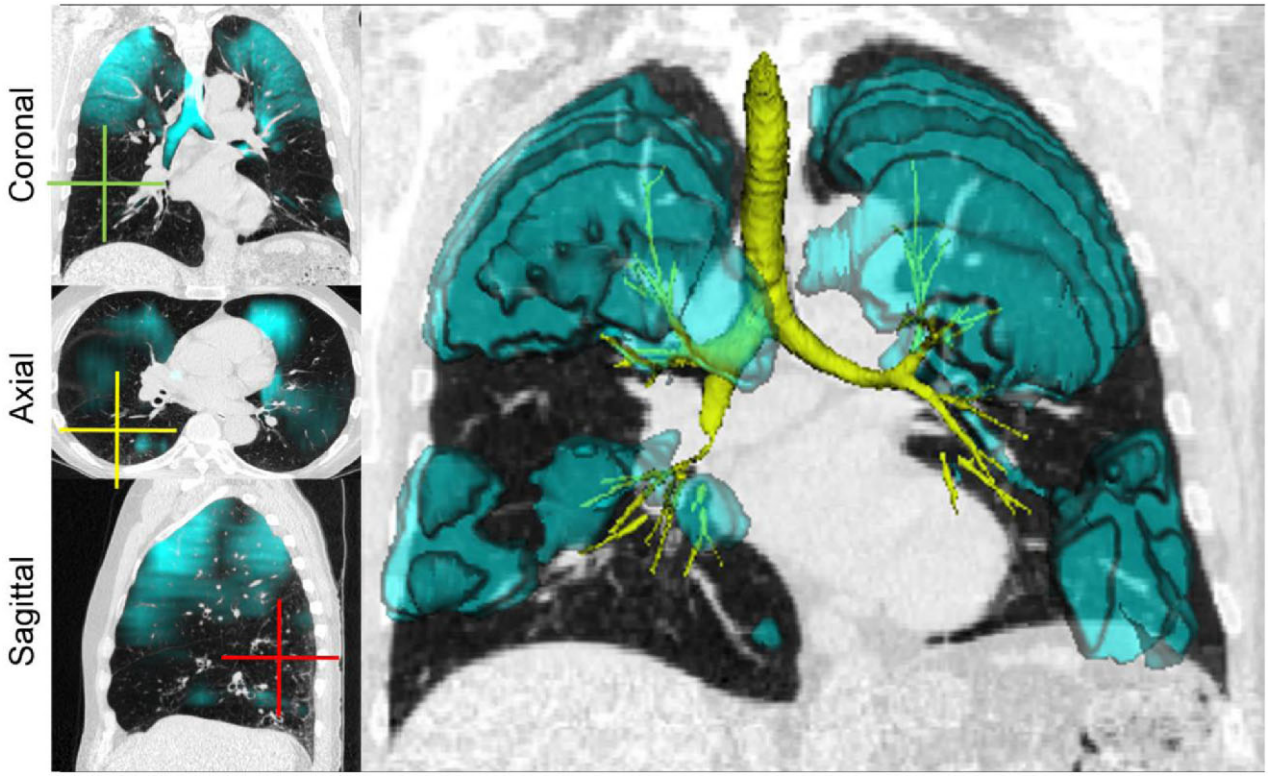

Figure 6 ^{3}He MRI ventilation defects and CT represent an emphysema dominant phenotype in chronic obstructive pulmonary disease. Three-dimensional co-registration of ^{3}He static ventilation (shown in blue) and CT density mask (RA_{950} map shown in yellow) highlights the emphysematous regions and airway tree segmented in brown.

and emphysematous human lungs,[84] revealed an abnormally increased ADC (tissue destruction) in emphysematous tissue. The use of these novel tools may prove very useful in α-one antitrypsin deficiency, especially in relation to replacement therapy.[85]

MRI AND CT COPD PHENOTYPES: CHALLENGE OR OPPORTUNITY?

In its current state, CT imaging provides anatomic imaging with acceptable spatial resolution and image quality. However, CT also includes a radiation burden that may be unacceptable in many circumstances (e.g. longitudinal monitoring). On the other hand, MRI provides both anatomical and functional images, without radiation burden, albeit with lower spatial resolution and in some cases, very poor image quality, compared to CT. For these reasons, the road towards a more complete understanding of COPD might include the complementary information provided by both methods. For example, as shown in Figures 6 and 7, both CT and MRI can be used in the research setting to deeply phenotype COPD patients based on quantitative lung structure and function. Figure 6 shows co-registered MRI and CT pulmonary data in a COPD patient who underwent both imaging methods within about 30 min, post-salbutamol. The spatial relationship between ventilation defects (MRI) and the airway tree (CT) of an airways disease-dominant COPD subject is shown in the axial, sagittal and coronal plane. Three-dimensional ventilation in transparent aqua is shown along with the airway tree to identify the direct airway tree-to-ventilation (structure–function) spatial relationships, which might prove important in specific interventions. As shown in the video, (https://youtu.be/7BFvssgt4zI) the large ventilation defect in the lower left lobe and corresponding airway and emphysema may be clearly identified for localized or targeted endobronchial interventions. However, it is also clear that this COPD ex-smoker has numerous ventilation abnormalities distributed in the right lung in addition to the larger left lower lobe abnormality. Furthermore, imaging provides a way to monitor and compare treatment responses in patients that have undergone bronchial thermoplasty, stent or valve placement. For example, a previous case study using ^{3}He MRI demonstrated the benefits of stent therapy in COPD.[86] However, further work is required to validate these observations in larger studies and to compare stents with other endobroncial interventions. Using this information, different COPD phenotypes may be identified that can potentially benefit from different endobronchial interventions.

Figure 7 provides an example of another ex-smoker with emphysema-dominant COPD and the direct spatial relationship between ventilation abnormalities and an emphysematous bulla (also shown in video https://youtu.be/T3IGV-9rAEY). This 3D view suggests that the airways leading to the ventilation

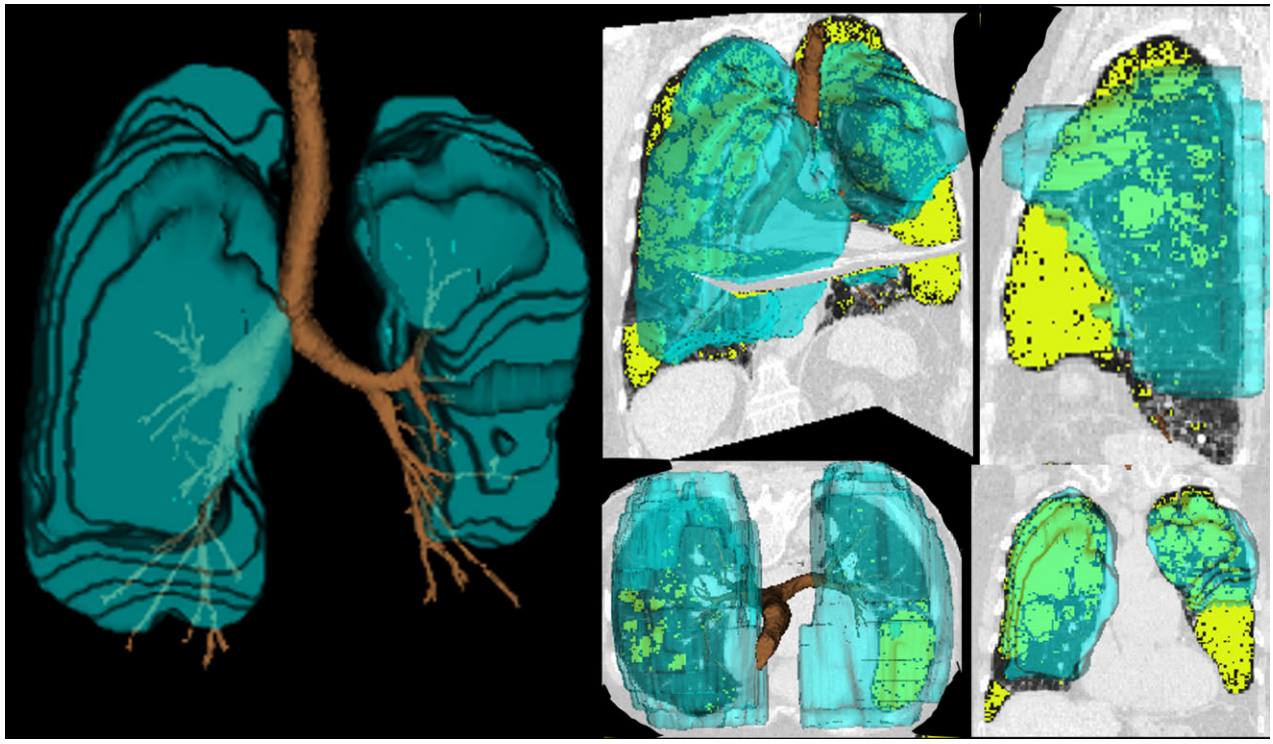

Figure 7 Spatial relationship between ^{3}He MRI ventilation defects and CT of a subject with airways disease dominant COPD. Co-registration of ^{3}He MRI static ventilation (shown in blue) and CT (shown in greyscale) with airway rendering (shown in yellow). A lower right lobe ventilation defect was identified and is shown in the coronal, axial and sagittal views.

defect are occluded and/or emphysema may be responsible for the ventilation defect because of long time-constants for lung filling in the bulla. In comparison to the ventilation defect shown in Figure 6, ventilation defects in Figure 7 are more homogeneously distributed, reflecting the fact that each COPD patient reflects a wide variety of airway, emphysema and ventilation patterns. We think these different 'looks' can be exploited in intervention trials and for individualized therapy decisions.

SUMMARY AND CONCLUSIONS

The use of CT and MRI in COPD research studies has evolved over last decades and[68,74] has provided new insights of the pathophysiology of COPD based on a visual and quantitative picture of the disease. Among its many strengths, CT is nearly universally available, images are rapidly acquired and because of the fundamental physics of X-ray-based methods, CT provides high spatial resolution measurements of lung structure that cannot be achieved using other functional imaging methods. However, for younger patients, even with low dose adaptive iteration methods, radiation dose and long-term burden/risk will always remain a concern for healthcare providers and for the patients themselves. MRI also provides quantitative measurements and novel insights about COPD lung structure and function without exposure to ionizing radiation, so it provides an excellent alternative when dose is a concern. While good agreement between MRI and CT measurements has been demonstrated, it is clear that MRI and CT methods provide different information that is very complementary.

Pulmonary function testing is widely accessible, easy to implement, and offers straightforward measurements that are validated for COPD disease progression and severity, but they do not tell the whole story for patient populations and individual patients. With the advancement of pulmonary imaging methods, there is growing evidence that different COPD patients with very similar pulmonary function measurements, experience the disease differently—greater or lesser symptoms and exercise capacities. As therapies begin to become more individualized, imaging may be the only way to quantify treatment response. Moreover, imaging may be the only way for us to see what COPD really looks like.

Acknowledgements

Dr. Parraga acknowledges funding (Operating, Team (Thoracic Imaging Network of Canada) and Network (Canadian Respiratory Research Network) and salary support (New Investigator Award) from the Canadian Institutes of Health Research. Dr. Coxson is support by a Roberta R. Miller Fellowship in Thoracic Imaging from the B.C. Lung Association. Ms. Sheikh's Ph.D. training stipend is funded by an award from the National Science and Engineering Research Council (Canada Graduate Scholarship-Doctoral).

REFERENCES

1 Hogg JC, Chu F, Utokaparch S, Woods R, Elliott WM, Buzatu L, Cherniack RM, Rogers RM, Sciurba FC, Coxson HO *et al.* The

nature of small-airway obstruction in chronic obstructive pulmonary disease. *N. Engl. J. Med.* 2004; **350**: 2645–53.
2 McDonough JE, Yuan R, Suzuki M, Seyednejad N, Elliott WM, Sanchez PG, Wright AC, Gefter WB, Litzky L, Coxson HO *et al*. Small-airway obstruction and emphysema in chronic obstructive pulmonary disease. *N. Engl. J. Med.* 2011; **365**: 1567–75.
3 Organization WH. *World health statistics 2010*. World Health Organization, Geneva, 2010.
4 Vestbo J, Hurd SS, Agusti AG, Jones PW, Vogelmeier C, Anzueto A, Barnes PJ, Fabbri LM, Martinez FJ, Nishimura M *et al*. Global strategy for the diagnosis, management, and prevention of chronic obstructive pulmonary disease: GOLD executive summary. *Am. J. Respir. Crit. Care Med.* 2013; **187**: 347–65.
5 Regan EA, Hokanson JE, Murphy JR, Make B, Lynch DA, Beaty TH, Curran-Everett D, Silverman EK, Crapo JD. Genetic epidemiology of COPD (COPDGene) study design. *COPD* 2010; **7**: 32–43.
6 Vestbo J, Anderson W, Coxson HO, Crim C, Dawber F, Edwards L, Hagan G, Knobil K, Lomas DA, MacNee W. Evaluation of COPD longitudinally to identify predictive surrogate end-points (ECLIPSE). *Eur. Respir. J.* 2008; **31**: 869–73.
7 Couper D, LaVange LM, Han MK, Barr RG, Bleecker ER, Hoffman EA, Kanner RE, Kleerup E, Martinez FJ, Woodruff PG *et al*. Design of the subpopulations and intermediate outcomes in COPD study (SPIROMICS). *Thorax* 2014; **69**: 491–4.
8 Lovasi GS, Diez Roux AV, Hoffman EA, Smith LJ, Jiang R, Carr JJ, Barr RG. Socioeconomic status is positively associated with per cent emphysema on CT scan: the MESA lung study. *Acad. Radiol.* 2011; **18**: 199–204.
9 Mitchell RS, Silvers GW, Goodman N, Dart G, Maisel JC. Are centrilobular emphysema and panlobular emphysema two different diseases? *Hum. Pathol.* 1970; **1**: 433–41.
10 Takahashi M, Fukuoka J, Nitta N, Takazakura R, Nagatani Y, Murakami Y, Otani H, Murata K. Imaging of pulmonary emphysema: a pictorial review. *Int. J. Chron. Obstruct. Pulmon. Dis.* 2008; **3**: 193–204.
11 Verschakelen JA, De Wever W. *Computed Tomography of the Lung: A Pattern Approach*. Springer Science & Business Media, Heidelberg, 2007.
12 Hounsfield GN. Radiography. Google Patents, 1978.
13 Litmanovich DE, Hartwick K, Silva M, Bankier AA. Multidetector computed tomographic imaging in chronic obstructive pulmonary disease: emphysema and airways assessment. *Radiol. Clin. North Am.* 2014; **52**: 137–54.
14 Sakai N, Mishima M, Nishimura K, Itoh H, Kuno K. An automated method to assess the distribution of low attenuation areas on chest CT scans in chronic pulmonary emphysema patients. *Chest* 1994; **106**: 1319–25.
15 Bankier AA, De Maertelaer V, Keyzer C, Gevenois PA. Pulmonary emphysema: subjective visual grading versus objective quantification with macroscopic morphometry and thin-section CT densitometry. *Radiology* 1999; **211**: 851–8.
16 Park KJ, Bergin CJ, Clausen JL. Quantitation of emphysema with three-dimensional CT densitometry: comparison with two-dimensional analysis, visual emphysema scores, and pulmonary function test results. *Radiology* 1999; **211**: 541–7.
17 Gevenois PA, de Maertelaer V, De Vuyst P, Zanen J, Yernault JC. Comparison of computed density and macroscopic morphometry in pulmonary emphysema. *Am. J. Respir. Crit. Care Med.* 1995; **152**: 653–7.
18 Muller NL, Staples CA, Miller RR, Abboud RT. 'Density mask'. An objective method to quantitate emphysema using computed tomography. *Chest* 1988; **94**: 782–7.
19 Coxson HO, Rogers RM, Whittall KP, D'Yachkova Y, Pare PD, Sciurba FC, Hogg JC. A quantification of the lung surface area in emphysema using computed tomography. *Am. J. Respir. Crit. Care Med.* 1999; **159**: 851–6.
20 Smith BM, Austin JH, Newell JD Jr, D'Souza BM, Rozenshtein A, Hoffman EA, Ahmed F, Barr RG. Pulmonary emphysema subtypes on computed tomography: the MESA COPD study. *Am. J. Med.* 2014; **127**: 94. e7–23.
21 Xu Y, Sonka M, McLennan G, Guo J, Hoffman EA. MDCT-based 3-D texture classification of emphysema and early smoking related lung pathologies. *IEEE Trans. Med. Imaging* 2006; **25**: 464–75.
22 Mishima M, Hirai T, Itoh H, Nakano Y, Sakai H, Muro S, Nishimura K, Oku Y, Chin K, Ohi M *et al*. Complexity of terminal airspace geometry assessed by lung computed tomography in normal subjects and patients with chronic obstructive pulmonary disease. *Proc. Natl. Acad. Sci. U.S.A.* 1999; **96**: 8829–34.
23 Madani A, Van Muylem A, de Maertelaer V, Zanen J, Gevenois PA. Pulmonary emphysema: size distribution of emphysematous spaces on multidetector CT images—comparison with macroscopic and microscopic morphometry. *Radiology* 2008; **248**: 1036–41.
24 Gietema HA, Muller NL, Fauerbach PV, Sharma S, Edwards LD, Camp PG, Coxson HO. Quantifying the extent of emphysema: factors associated with radiologists' estimations and quantitative indices of emphysema severity using the ECLIPSE cohort. *Acad. Radiol.* 2011; **18**: 661–71.
25 Sorensen L, Shaker SB, de Bruijne M. Quantitative analysis of pulmonary emphysema using local binary patterns. *IEEE Trans. Med. Imaging* 2010; **29**: 559–69.
26 Owrangi AM, Etemad-Rezai R, McCormack DG, Cunningham IA, Parraga G. Computed tomography density histogram analysis to evaluate pulmonary emphysema in ex-smokers. *Acad. Radiol.* 2013; **20**: 537–45.
27 Okazawa M, Muller N, McNamara AE, Child S, Verburgt L, Pare PD. Human airway narrowing measured using high resolution computed tomography. *Am. J. Respir. Crit. Care Med.* 1996; **154**: 1557–62.
28 Tschirren J, Hoffman EA, McLennan G, Sonka M. Intrathoracic airway trees: segmentation and airway morphology analysis from low-dose CT scans. *IEEE Trans. Med. Imaging* 2005; **24**: 1529–39.
29 Nakano Y, Wong JC, de Jong PA, Buzatu L, Nagao T, Coxson HO, Elliott WM, Hogg JC, Pare PD. The prediction of small airway dimensions using computed tomography. *Am. J. Respir. Crit. Care Med.* 2005; **171**: 142–6.
30 Nakano Y, Muro S, Sakai H, Hirai T, Chin K, Tsukino M, Nishimura K, Itoh H, Pare PD, Hogg JC *et al*. Computed tomographic measurements of airway dimensions and emphysema in smokers. Correlation with lung function. *Am. J. Respir. Crit. Care Med.* 2000; **162**: 1102–8.
31 Han MK, Kazerooni EA, Lynch DA, Liu LX, Murray S, Curtis JL, Criner GJ, Kim V, Bowler RP, Hanania NA *et al*. Chronic obstructive pulmonary disease exacerbations in the COPDGene study: associated radiologic phenotypes. *Radiology* 2011; **261**: 274–82.
32 Grydeland TB, Dirksen A, Coxson HO, Eagan TM, Thorsen E, Pillai SG, Sharma S, Eide GE, Gulsvik A, Bakke PS. Quantitative computed tomography measures of emphysema and airway wall thickness are related to respiratory symptoms. *Am. J. Respir. Crit. Care Med.* 2010; **181**: 353–9.
33 Orlandi I, Moroni C, Camiciottoli G, Bartolucci M, Pistolesi M, Villari N, Mascalchi M. Chronic obstructive pulmonary disease: thin-section CT measurement of airway wall thickness and lung attenuation. *Radiology* 2005; **234**: 604–10.
34 Kim V, Desai P, Newell JD, Make BJ, Washko GR, Silverman EK, Crapo JD, Bhatt SP, Criner GJ. Airway wall thickness is increased in COPD patients with bronchodilator responsiveness. *Respir. Res.* 2014; **15**: 84–93.
35 Smith BM, Hoffman EA, Rabinowitz D, Bleecker E, Christenson S, Couper D, Donohue KM, Han MK, Hansel NN, Kanner RE *et al*. Comparison of spatially matched airways reveals thinner airway walls in COPD. The multi-ethnic study of atherosclerosis (MESA) COPD study and the subpopulations and intermediate outcomes in COPD study (SPIROMICS). *Thorax* 2014; **69**: 987–96.

36 Suzuki T, Tada Y, Kawata N, Matsuura Y, Ikari J, Kasahara Y, Tatsumi K. Clinical, physiological, and radiological features of asthma-chronic obstructive pulmonary disease overlap syndrome. *Int. J. Chron. Obstruct. Pulmon. Dis.* 2015; **10**: 947–54.

37 Sieren JP, Newell JD, Judy PF, Lynch DA, Chan KS, Guo J, Hoffman EA. Reference standard and statistical model for intersite and temporal comparisons of CT attenuation in a multicenter quantitative lung study. *Med. Phys.* 2012; **39**: 5757–67.

38 Hoffman EA, Barr R. Thresholds to lung density measures. Hoffman and Barr replies. *Acad. Radiol* 2010; **17**: 339–401.

39 Galban CJ, Han MK, Boes JL, Chughtai KA, Meyer CR, Johnson TD, Galban S, Rehemtulla A, Kazerooni EA, Martinez FJ *et al*. Computed tomography-based biomarker provides unique signature for diagnosis of COPD phenotypes and disease progression. *Nat. Med.* 2012; **18**: 1711–15.

40 Park EA, Goo JM, Park SJ, Lee HJ, Lee CH, Park CM, Yoo CG, Kim JH. Chronic obstructive pulmonary disease: quantitative and visual ventilation pattern analysis at xenon ventilation CT performed by using a dual-energy technique. *Radiology* 2010; **256**: 985–97.

41 Guerrero T, Sanders K, Castillo E, Zhang Y, Bidaut L, Pan T, Komaki R. Dynamic ventilation imaging from four-dimensional computed tomography. *Phys. Med. Biol.* 2006; **51**: 777–91.

42 Mathew L, Wheatley A, Castillo R, Castillo E, Rodrigues G, Guerrero T, Parraga G. Hyperpolarized (3)He magnetic resonance imaging: comparison with four-dimensional x-ray computed tomography imaging in lung cancer. *Acad. Radiol.* 2012; **19**: 1546–53.

43 Jahani N, Yin Y, Hoffman EA, Lin CL. Assessment of regional non-linear tissue deformation and air volume change of human lungs via image registration. *J. Biomech.* 2014; **47**: 1626–33.

44 Mannino DM, Buist AS. Global burden of COPD: risk factors, prevalence, and future trends. *Lancet* 2007; **370**: 765–73.

45 Lundback B, Lindberg A, Lindstrom M, Ronmark E, Jonsson AC, Jonsson E, Larsson LG, Andersson S, Sandstrom T, Larsson K. Not 15 but 50% of smokers develop COPD?—Report from the obstructive lung disease in Northern Sweden studies. *Respir. Med.* 2003; **97**: 115–22.

46 Hoffman EA, Simon BA, McLennan G. State of the art. A structural and functional assessment of the lung via multidetector-row computed tomography: phenotyping chronic obstructive pulmonary disease. *Proc. Am. Thorac. Soc.* 2006; **3**: 519–32.

47 Alford SK, van Beek EJ, McLennan G, Hoffman EA. Heterogeneity of pulmonary perfusion as a mechanistic image-based phenotype in emphysema susceptible smokers. *Proc. Natl. Acad. Sci. U.S.A.* 2010; **107**: 7485–90.

48 Jang YM, Oh YM, Seo JB, Kim N, Chae EJ, Lee YK, Lee SD. Quantitatively assessed dynamic contrast-enhanced magnetic resonance imaging in patients with chronic obstructive pulmonary disease: correlation of perfusion parameters with pulmonary function test and quantitative computed tomography. *Invest. Radiol.* 2008; **43**: 403–10.

49 Alford S, van Beek E, Hudson M, Baumhauer H, McLennan G, Hoffman E. Characterization of regional alterations in pulmonary perfusion via MDCT in nonsmokers and smokers. *Eur. Radiol.* 2008; **18**: 330–1.

50 Vogel-Claussen J, Renne J, Hinrichs J, Schonfeld C, Gutberlet M, Schaumann F, Winkler C, Faulenbach C, Krug N, Wacker FK *et al*. Quantification of pulmonary inflammation after segmental allergen challenge using TIRM magnetic resonance imaging. *Am. J. Respir. Crit. Care Med.* 2014; **189**: 650–7.

51 Ley-Zaporozhan J, Ley S, Kauczor HU. Proton MRI in COPD. *COPD* 2007; **4**: 55–65.

52 Ohno Y, Koyama H, Yoshikawa T, Matsumoto K, Takahashi M, Van Cauteren M, Sugimura K. T2* measurements of 3-T MRI with ultrashort TEs: capabilities of pulmonary function assessment and clinical stage classification in smokers. *AJR Am. J. Roentgenol.* 2011; **197**: W279–85.

53 Ma W, Sheikh K, Svenningsen S, Pike D, Guo F, Etemad-Rezai R, Leipsic J, Coxson HO, McCormack DG, Parraga G. Ultra-short echo-time pulmonary MRI: evaluation and reproducibility in COPD subjects with and without bronchiectasis. *J. Magn. Reson. Imaging* 2015; **41**: 1465–74.

54 Mayo JR. Thoracic magnetic resonance imaging: physics and pulse sequences. *J. Thorac. Imaging* 1993; **8**: 1–11.

55 Takahashi M, Togao O, Obara M, van Cauteren M, Ohno Y, Doi S, Kuro-o M, Malloy C, Hsia CC, Dimitrov I. Ultra-short echo time (UTE) MR imaging of the lung: comparison between normal and emphysematous lungs in mutant mice. *J. Magn. Reson. Imaging* 2010; **32**: 326–33.

56 Zurek M, Boyer L, Caramelle P, Boczkowski J, Crémillieux Y. Longitudinal and noninvasive assessment of emphysema evolution in a murine model using proton MRI. *Magn. Reson. Med.* 2012; **68**: 898–904.

57 Stadler A, Jakob PM, Griswold M, Stiebellehner L, Barth M, Bankier AA. T1 mapping of the entire lung parenchyma: influence of respiratory phase and correlation to lung function test results in patients with diffuse lung disease. *Magn. Reson. Med.* 2008; **59**: 96–101.

58 Bauman G, Puderbach M, Deimling M, Jellus V, Chefd'hotel C, Dinkel J, Hintze C, Kauczor HU, Schad LR. Non-contrast-enhanced perfusion and ventilation assessment of the human lung by means of Fourier decomposition in proton MRI. *Magn. Reson. Med.* 2009; **62**: 656–64.

59 Capaldi DP, Sheikh K, Guo F, Svenningsen S, Etemad-Rezai R, Coxson HO, Leipsic JA, McCormack DG, Parraga G. Free-breathing pulmonary 1H and hyperpolarized 3He MRI: comparison in COPD and bronchiectasis. *Acad. Radiol.* 2015; **22**: 320–9.

60 Lederlin M, Bauman G, Eichinger M, Dinkel J, Brault M, Biederer J, Puderbach M. Functional MRI using Fourier decomposition of lung signal: reproducibility of ventilation- and perfusion-weighted imaging in healthy volunteers. *Eur. J. Radiol.* 2013; **82**: 1015–22.

61 Zurek M, Johansson E, Risse F, Alamidi D, Olsson LE, Hockings PD. Accurate T(1) mapping for oxygen-enhanced MRI in the mouse lung using a segmented inversion-recovery ultrashort echo-time sequence. *Magn. Reson. Med.* 2014; **71**: 2180–5.

62 Edelman RR, Hatabu H, Tadamura E, Li W, Prasad PV. Noninvasive assessment of regional ventilation in the human lung using oxygen-enhanced magnetic resonance imaging. *Nat. Med.* 1996; **2**: 1236–9.

63 Muller CJ, Schwaiblmair M, Scheidler J, Deimling M, Weber J, Loffler RB, Reiser MF. Pulmonary diffusing capacity: assessment with oxygen-enhanced lung MR imaging preliminary findings. *Radiology* 2002; **222**: 499–506.

64 Halaweish AF, Moon RE, Foster WM, Soher BJ, McAdams HP, MacFall JR, Ainslie MD, MacIntyre NR, Charles HC. Perfluoropropane gas as a magnetic resonance lung imaging contrast agent in humans. *Chest* 2013; **144**: 1300–10.

65 Couch MJ, Ball IK, Li T, Fox MS, Littlefield SL, Biman B, Albert MS. Pulmonary ultrashort echo time 19F MR imaging with inhaled fluorinated gas mixtures in healthy volunteers: feasibility. *Radiology* 2013; **269**: 903–9.

66 Kirby M, Heydarian M, Svenningsen S, Wheatley A, McCormack DG, Etemad-Rezai R, Parraga G. Hyperpolarized 3He magnetic resonance functional imaging semiautomated segmentation. *Acad. Radiol.* 2012; **19**: 141–52.

67 Svenningsen S, Kirby M, Starr D, Leary D, Wheatley A, Maksym GN, McCormack DG, Parraga G. Hyperpolarized (3)He and (129)Xe MRI: differences in asthma before bronchodilation. *J. Magn. Reson. Imaging* 2013; **38**: 1521–30.

68 Kirby M, Pike D, Coxson HO, McCormack DG, Parraga G. Hyperpolarized (3)He ventilation defects used to predict pulmonary exacerbations in mild to moderate chronic obstructive pulmonary disease. *Radiology* 2014; **273**: 887–96.

69 Mathew L, Kirby M, Etemad-Rezai R, Wheatley A, McCormack DG, Parraga G. Hyperpolarized (3)He magnetic resonance imaging: preliminary evaluation of phenotyping potential in

chronic obstructive pulmonary disease. *Eur. J. Radiol.* 2011; **79**: 140–6.
70 Woods JC, Choong CK, Yablonskiy DA, Bentley J, Wong J, Pierce JA, Cooper JD, Macklem PT, Conradi MS, Hogg JC. Hyperpolarized 3He diffusion MRI and histology in pulmonary emphysema. *Magn. Reson. Med.* 2006; **56**: 1293–300.
71 Salerno M, de Lange EE, Altes TA, Truwit JD, Brookeman JR, Mugler JP. Emphysema: hyperpolarized helium 3 diffusion MR imaging of the lungs compared with spirometric indexes—initial experience. *Radiology* 2002; **222**: 252–60.
72 Fain SB, Altes TA, Panth SR, Evans MD, Waters B, Mugler JP 3rd, Korosec FR, Grist TM, Silverman M, Salerno M *et al*. Detection of age-dependent changes in healthy adult lungs with diffusion-weighted 3He MRI. *Acad. Radiol.* 2005; **12**: 1385–93.
73 Fain SB, Panth SR, Evans MD, Wentland AL, Holmes JH, Korosec FR, O'Brien MJ, Fountaine H, Grist TM. Early emphysematous changes in asymptomatic smokers: detection with 3He MR imaging. *Radiology* 2006; **239**: 875–83.
74 Kirby M, Owrangi A, Svenningsen S, Wheatley A, Coxson HO, Paterson NA, McCormack DG, Parraga G. On the role of abnormal DLCO in ex-smokers without airflow limitation: symptoms, exercise capacity and hyperpolarised helium-3 MRI. *Thorax* 2013; **68**: 752–9.
75 Kaushik SS, Cleveland ZI, Cofer GP, Metz G, Beaver D, Nouls J, Kraft M, Auffermann W, Wolber J, McAdams HP *et al*. Diffusion-weighted hyperpolarized 129Xe MRI in healthy volunteers and subjects with chronic obstructive pulmonary disease. *Magn. Reson. Med.* 2011; **65**: 1154–65.
76 Kirby M, Svenningsen S, Owrangi A, Wheatley A, Farag A, Ouriadov A, Santyr GE, Etemad-Rezai R, Coxson HO, McCormack DG *et al*. Hyperpolarized 3He and 129Xe MR imaging in healthy volunteers and patients with chronic obstructive pulmonary disease. *Radiology* 2012; **265**: 600–10.
77 Milic-Emili J. Radioactive xenon in the evaluation of regional lung function. *Semin. Nucl. Med.* 1971; **1**: 246–62.
78 Driehuys B, Cofer GP, Pollaro J, Mackel JB, Hedlund LW, Johnson GA. Imaging alveolar-capillary gas transfer using hyperpolarized 129Xe MRI. *Proc. Natl. Acad. Sci. U.S.A.* 2006; **103**: 18278–83.
79 Yablonskiy DA, Sukstanskii AL, Leawoods JC, Gierada DS, Bretthorst GL, Lefrak SS, Cooper JD, Conradi MS. Quantitative in vivo assessment of lung microstructure at the alveolar level with hyperpolarized 3He diffusion MRI. *Proc. Natl. Acad. Sci. U.S.A.* 2002; **99**: 3111–16.
80 Quirk JD, Chang YV, Yablonskiy DA. In vivo lung morphometry with hyperpolarized (3) He diffusion MRI: reproducibility and the role of diffusion-sensitizing gradient direction. *Magn. Reson. Med.* 2015; **73**: 1252–7.
81 Sukstanskii AL, Yablonskiy DA. In vivo lung morphometry with hyperpolarized 3 He diffusion MRI: theoretical background. *J. Magn. Reson.* 2008; **190**: 200–10.
82 Ouriadov A, Farag A, Kirby M, McCormack DG, Parraga G, Santyr GE. Lung morphometry using hyperpolarized (129) Xe apparent diffusion coefficient anisotropy in chronic obstructive pulmonary disease. *Magn. Reson. Med.* 2013; **70**: 1699–706.
83 Carrero-Gonzalez L, Kaulisch T, Stiller D. In vivo diffusion-weighted MRI using perfluorinated gases: ADC comparison between healthy and elastase-treated rat lungs. *Magn. Reson. Med.* 2013; **70**: 1761–4.
84 Jacob RE, Chang YV, Choong CK, Bierhals A, Zheng Hu D, Zheng J, Yablonskiy DA, Woods JC, Gierada DS, Conradi MS. 19F MR imaging of ventilation and diffusion in excised lungs. *Magn. Reson. Med.* 2005; **54**: 577–85.
85 Wood AM, Stockley RA. Alpha one antitrypsin deficiency: from gene to treatment. *Respiration* 2007; **74**: 481–92.
86 Mathew L, Kirby M, Farquhar D, Licskai C, Santyr G, Etemad-Rezai R, Parraga G, McCormack DG. Hyperpolarized 3He functional magnetic resonance imaging of bronchoscopic airway bypass in chronic obstructive pulmonary disease. *Can. Respir. J.* 2012; **19**: 41–3.

